DRAFT VERSION DECEMBER 21, 2010
Preprint typeset using LaTeX style emulateapj v. 03/07/07

arXiv:1012.4009v1 [astro-ph.HE] 17 Dec 2010

THE OPTICAL AFTERGLOW AND $z = 0.92$ EARLY-TYPE HOST GALAXY OF THE SHORT GRB 100117A

W. FONG[1], E. BERGER[1], R. CHORNOCK[1], N.R. TANVIR[2], A.J. LEVAN[3], A.S. FRUCHTER[4], J.F. GRAHAM[4], A. CUCCHIARA[5], D.B. FOX[6]

Draft version December 21, 2010

ABSTRACT

We present the discovery of the optical afterglow and early-type host galaxy of the short-duration GRB 100117A. The faint afterglow is detected 8.3 hr after the burst with $r_{\rm AB} = 25.46 \pm 0.20$ mag. Follow-up optical and near-IR observations uncover a coincident compact red galaxy, identified as an early-type galaxy at a photometric redshift of $z \approx 0.6-0.9$ (2σ) with a mass of $\sim 3 \times 10^{10}$ M$_\odot$, an age of ~ 1 Gyr, and a luminosity of $L_B \simeq 0.5 L_*$. Spectroscopic observations of the host reveal a notable break corresponding to the Balmer/4000Å break at $z \approx 0.9$, and stellar population spectral evolution template fits indicate $z \approx 0.915$, which we adopt as the redshift of the host, with stellar population ages of $\sim 1-3$ Gyr. From a possible weak detection of [O II]λ3727 emission at $z = 0.915$ we infer an upper bound on the star formation rate of ~ 0.1 M$_\odot$ yr^{-1}, leading to a specific star formation rate of $\lesssim 0.004$ Gyr^{-1}. Thus, GRB 100117A is only the second short burst to date with a secure early-type host (the other being GRB 050724 at $z = 0.257$) and it has one of the highest short GRB redshifts. The offset between the host center and the burst position, 470 ± 310 pc, is the smallest to date. Combined with the old stellar population age, this indicates that the burst likely originated from a progenitor with no significant kick velocity. However, from the brightness of the optical afterglow we infer a relatively low density of $n \approx 3 \times 10^{-4} \epsilon_{e,-1}^{-3} \epsilon_{B,-1}^{-1.75}$ cm^{-3}. The combination of an optically faint afterglow and host suggest that previous such events may have been missed, thereby potentially biasing the known short GRB host population against $z \gtrsim 1$ early-type hosts.

Subject headings: gamma-rays:bursts

1. INTRODUCTION

Progress in our understanding of short-duration gamma-ray bursts (GRBs) and their progenitors relies on detailed studies of their afterglows and host galaxy environments. Of particular interest are bursts with precise sub-arcsecond positions, which can provide unambiguous host galaxy associations, redshifts, and burst properties (energy, density). Such localizations require the detection of ultraviolet, optical, near-infrared, and/or radio afterglows; or alternatively an X-ray detection with the *Chandra* X-ray Observatory. As of December 2010, only 20 short bursts have been precisely localized in this manner. Of these, 14 have clearly identified hosts[7] (10 with spectroscopic redshifts), 5 do not have unambiguous host associations[8] (Berger 2010a), and 1 has not been reported in the literature so far[9]. For a recent summary see Berger (2010b).

Only in a single case out of the 10 hosts with spectroscopic identifications is the galaxy known to be early-type with no evidence for on-going star formation activity (GRB 050724: Berger et al. 2005); the remaining hosts are star forming galaxies, albeit at a level that is on average significantly lower than in long GRB hosts (Berger 2009), particularly when accounting for their higher luminosities and stellar masses (Berger 2009; Leibler & Berger 2010). The hosts with measured redshifts span a range of $z \approx 0.1-1$ (e.g., Berger 2009), with the exception of GRB 090426 at $z = 2.609$ (Antonelli et al. 2009; Levesque et al. 2010); in the three remaining cases the hosts are too faint for a spectroscopic redshift determination, but are likely to be located at $z \gtrsim 1$ (Berger et al. 2007a). At the same time, there is tentative evidence for early-type hosts in the sample of short bursts with optical positions and no coincident hosts based on chance coincidence probabilities (GRBs 070809 and 090515; Berger 2010a).

The host demographics and redshift distribution provide important constraints on the nature of the progenitors. For example, an abundance of low redshifts and early-type hosts would point to a population that is skewed to old ages, $\gtrsim$ few Gyr (Zheng & Ramirez-Ruiz 2007). However, from the existing host galaxy demographics and redshift distributions it appears that the progenitors span a broad range of ages, $\sim 0.1-$ few Gyr, and may indeed be over-represented in late-type galaxies with intermediate-age populations (~ 0.3 Gyr; Berger et al. 2007a; Leibler & Berger 2010).

Afterglow detections are also important for determining the GRB and circumburst medium properties. To date, however, little detailed information about these properties has been drawn from the existing (though sparse) broad-band af-

[1] Harvard-Smithsonian Center for Astrophysics, 60 Garden Street, Cambridge, MA 02138
[2] Department of Physics and Astronomy, University of Leicester, University Road, Leicester LE1 7RH, UK
[3] Department of Physics, University of Warwick, Coventry, CV4 7AL, UK
[4] Space Telescope Science Institute, 3700 San Martin Drive, Baltimore, MD 21218
[5] Lawrence Berkeley National Laboratory, MS 50B-4026, 1 Cyclotron Road, Berkeley, CA, 94720
[6] Department of Astronomy and Astrophysics, 525 Davey Laboratory, Pennsylvania State University, University Park, PA 16802

[7] These bursts are 050709: (Fox et al. 2005; Hjorth et al. 2005b); 050724: (Berger et al. 2005); 051221A: (Soderberg et al. 2006); 060121 (Levan et al. 2006; de Ugarte Postigo et al. 2006); 060313: (Roming et al. 2006); 061006: (D'Avanzo et al. 2009); 070707: (Piranomonte et al. 2008); 070714B: (Graham et al. 2009); 070724: (Berger et al. 2009); 071227: (D'Avanzo et al. 2009); 080905: (Rowlinson et al. 2010a); 090426: (Antonelli et al. 2009; Levesque et al. 2010); 090510: (McBreen et al. 2010); and 100117A: this paper.

[8] GRBs 061201: (Stratta et al. 2007), 070809: (Perley et al. 2007), 080503: (Perley et al. 2009), 090305: (Berger & Kelson 2009; Cenko et al. 2009), and 090515: (Rowlinson et al. 2010b).

[9] GRB 091109b: (Malesani et al. 2009).

terglow detections (e.g., Berger et al. 2005; Panaitescu 2006; Roming et al. 2006; Soderberg et al. 2006; Berger 2010a), mainly due to the faintness of short GRB afterglows. Early time optical observations also probe possible emission from radioactive material synthesized and ejected in a binary compact object merger, a so-called Li-Paczynski mini-supernova (Li & Paczyński 1998; Metzger et al. 2010). No such emission has been conclusively detected to date (e.g., Hjorth et al. 2005a; Bloom et al. 2006; Berger et al. 2009).

Here we report the discovery of the optical afterglow and host galaxy of the short GRB 100117A. From spectroscopy and optical/near-IR imaging we find that the host is an early-type galaxy at $z = 0.915$, making it only the second unambiguous early-type host association for a short GRB with a significantly higher redshift than the previous event, GRB 050724 at $z = 0.257$ (Berger et al. 2005). The precise position also allows us to measure the burst offset, while the optical flux provides constraints on the circumburst density. We present the afterglow and host discovery in §2. In §3 we study the host redshift and stellar population properties, while in §4 we analyze the afterglow properties. Finally, we draw conclusions about the nature of this burst and implications for the short GRB sample in §5.

Throughout the paper we use the standard cosmological parameters, $H_0 = 71$ km s^{-1} Mpc^{-1}, $\Omega_m = 0.27$, and $\Omega_\Lambda = 0.73$.

2. OBSERVATIONS OF GRB 100117A

GRB 100117A was detected by the *Swift* satellite on 2010 January 17.879 UT, and an X-ray counterpart was promptly localized by the on-board X-ray Telescope (XRT) with a final positional accuracy of 2.4″ radius (de Pasquale et al. 2010). No optical/UV source was detected by the co-aligned UV/Optical Telescope (UVOT). The burst duration is $T_{90} = 0.30 \pm 0.05$ s, and its $15-150$ keV fluence is $F_\gamma = (9.3 \pm 1.3) \times 10^{-8}$ erg cm^{-2}. The burst was also detected by the *Fermi* Gamma-Ray Burst Monitor (GBM) with a duration of about 0.4 s, an $8-1000$ keV fluence of $F_\gamma = (4.1 \pm 0.5) \times 10^{-7}$ erg cm^{-2}, and a peak energy of $E_p = 287^{+74}_{-50}$ keV (de Pasquale et al. 2010). These properties clearly classify GRB 100117A as a short burst.

The X-ray light curve exhibits a complex behavior at early time, with an initial flare lasting until about 200 s, followed by a steep decline with $F_X \propto t^{-3.5\pm0.2}$. Subsequent data collected at $\sim 5-690$ ks lead to an upper limit of $F_X \lesssim 2.5 \times 10^{-14}$ erg cm^{-2} s^{-1} (unabsorbed; Evans et al. 2007, 2009). A fit to the X-ray spectrum indicates that $F_X \propto \nu^{-0.70\pm0.14}$ and $N_H = (1.2 \pm 0.4) \times 10^{21}$ cm^{-2}, in excess of the expected Galactic column of $N_H = 2.7 \times 10^{20}$ cm^{-2} (de Pasquale et al. 2010). Using the counts to unabsorbed flux conversion (1 cps $= 5.2 \times 10^{-11}$ erg cm^{-2} s^{-1}) and the measured spectral index, we find a flux density limit at $\gtrsim 5$ ks of $F_\nu(1\,\mathrm{keV}) \lesssim 2.3 \times 10^{-3}$ μJy.

Ground-based follow-up optical observations of the XRT position were first obtained with the Nordic Optical Telescope (NOT) 20.4 min after the burst and led to the marginal detection of a source with $R \approx 22.5$ mag (Xu et al. 2010). Inspection of archival optical images from the Canada-France-Hawaii MegaCam survey led to the detection of four faint sources within the initial XRT error circle with $R, I \approx 23-24.5$ mag, while *i*-band imaging at about 4.7 hr revealed that the brightest of these sources had a comparable brightness to the archival data and was likely the same source detected by Xu et al. 2010 (Cenko et al. 2010).

2.1. *Afterglow Discovery*

We initiated *R*-band observations of GRB 100117A with the Inamori Magellan Areal Camera and Spectrograph (IMACS) on the Magellan/Baade 6.5-m telescope on 2010 January 18.04 UT (3.9 hr after the burst) and detected the four sources noted by Cenko et al. (2010) within the initial XRT error circle. We subsequently obtained two deeper epochs of imaging in the *r*-band with the Gemini Multi-Object Spectrograph (GMOS-N) on the Gemini-North 8-m telescope on 2010 January 18.21 and 19.22 UT (7.9 and 33.2 hr after the burst); see Table 1. The IMACS observations were reduced using standard procedures in IRAF, while the GMOS-N observations were analyzed using the IRAF `gemini` package.

Digital image subtraction of the two GMOS-N observations using the ISIS software package (Alard 2000) reveals the presence of a fading source, which we identify as the optical afterglow of GRB 100117A; see Figure 1. Assuming that the afterglow contribution is negligible in the second GMOS-N observation we calculate a magnitude of $r_{\rm AB} = 25.46 \pm 0.20$ mag (0.24 ± 0.05 μJy) at a median time of 8.3 hr after the burst. A comparison of our IMACS observation with the second epoch of GMOS-N imaging yields an afterglow magnitude of $r_{\rm AB} > 23.93$ mag (3σ) at a median time of 4.1 hr after the burst.

Astrometry relative to the USNO-B catalog provides an absolute position for the optical afterglow of $\alpha = 00^{\rm h}45^{\rm m}04.660^{\rm s}$, $\delta = -01^\circ35'41.89''$ (J2000), with an uncertainty of 0.26″ in each coordinate. This position is 1.5″ away from the center of the XRT error circle, which has an uncertainty of 2.4″. We additionally measure the relative position of the afterglow and host galaxy (using the second Gemini epoch) and find an offset of δRA = 60 mas and δDec = 0 mas. The uncertainty in the offset includes contributions from the astrometric tie of the two Gemini observations ($\sigma_{\rm GB\to GB} = 9$ mas), the positional accuracy of the afterglow residual ($\sigma_{\theta,\rm GRB} = 10$ mas), and uncertainty in the centroid of the host galaxy ($\sigma_{\theta,\rm gal} = 20$), which is itself dominated by systematic uncertainty rather than just the signal-to-noise ratio. Thus, the total angular offset between the afterglow and host center is 60 ± 40 mas.

2.2. *Host Galaxy Observations*

Subsequent to the discovery of the afterglow we obtained follow-up observations of the host galaxy in the *g*-band with GMOS-N and in the *JHK* bands with the Near Infra-Red Imager and Spectrometer (NIRI) on the Gemini-North 8-m telescope. We also obtained IMACS observations in the *riz* bands (Table 1). Photometry of the host was extracted in a 1.6″ radius aperture, and is summarized in Table 1. We note that the errors are dominated by uncertainty in the zeropoint in the *H* and *K* bands. The host appears to be mildly resolved with a FWHM of 0.6″ in the *K*-band (PSF = 0.5″). Images of the host in the *grizJHK* filters, and a combined color image are shown in Figure 2. A combined color image of the 2′ field covered by NIRI is shown in Figure 3.

We obtained spectroscopic observations of the host on 2010 January 19.22 using GMOS-N at a mean airmass of 1.4. A dithered pair of 1500 s exposures were obtained with the R400 grating covering $3900-8130$ Å at a spectral resolution of about 7 Å. We obtained a second, deeper set of observations (4×1460 s) on 2010 November 2.12 with GMOS-S on the Gemini-South 8-m telescope at a mean airmass of 1.15 in the nod-and-shuffle mode. These observations were also obtained with the R400 grating covering $5400-9650$ Å with the OG515 order-blocking filter. The data were reduced using

standard tasks in IRAF and wavelength calibration was performed using CuAr arc lamps. Archival observations of the smooth-spectrum standard star EG 131 (Bessell 1999) and custom IDL programs were used to apply a flux calibration and remove the telluric absorption bands. In order to maximize the signal-to-noise ratio, we use a weighted co-addition of the two epochs in our subsequent analysis. The resulting spectrum is shown in Figure 4.

We detect continuum emission from the host beyond $\approx$ 5000 Å, with a notable increase in the flux redward of 7650 Å. No obvious emission features are detected. Interpreting the break as the Balmer/4000Å break we find an estimated redshift of $z \approx 0.9$.

3. HOST GALAXY REDSHIFT AND PROPERTIES

3.1. *Spectroscopy*

To quantitatively assess the host galaxy's redshift, we fit a weighted co-addition of the GMOS spectra described in §2.2 over the wavelength range 6000 – 8500 Å with spectral evolution models of simple stellar populations (SSPs) provided as part of the GALAXEV library (Bruzual & Charlot 2003); at wavelengths outside this range, the signal-to-noise ratio is too low to contribute significantly to the fit. We use χ^2 minimization with redshift as the free parameter and the best-fit flux normalization determined by the equation,

$$F_{0,\rm bf} = \frac{\sum_{i=1}^{n} \frac{F_{\lambda,model,i} \times F_{\lambda,gal,i}}{\sigma^2_{\lambda,gal,i}}}{\sum_{i=1}^{n} \frac{F^2_{\lambda,model,i}}{\sigma^2_{\lambda,gal,i}}}, \quad (1)$$

where $F_{\lambda,model,i}$ are the model fluxes, and $F_{\lambda,gal,i}$ and $\sigma_{\lambda,gal,i}$ are the observed galaxy fluxes and uncertainties, respectively. The fit is performed on the unbinned data. The resulting best-fit redshift is $z = 0.915$ ($\chi^2_\nu = 1.26$ for 1841 degrees of freedom at 1.4 Gyr) for SSPs with an age of 0.9 – 2.5 Gyr; see Figure 4. Significantly poorer fits are found with SSPs outside of this age range, or with late-type templates. At this redshift, there is a clear match between absorption features in the spectrum and the expected dominant lines (i.e., Ca II H&K, Mg I, and G-band). The distribution of χ^2_ν as a function of redshift is shown in Figure 5 revealing a secondary broad minimum at $z \approx 0.75$. This solution provides a much poorer fit to the data with $\chi^2_\nu = 1.60$, corresponding to about 10σ away from the best fit. The main reason for the poor fit is that it misses the key spectral absorption features and the clear break at 7650 Å (Figure 4).

At the best-fit spectroscopic redshift of $z = 0.915$ we find a marginal feature corresponding to [O II]λ3727 with a flux of $F_{\rm [OII]} \approx 3 \times 10^{-18}$ erg cm^{-2} s^{-1}, or $L_{\rm [OII]} \approx 7 \times 10^{39}$ erg s^{-1}. Given the marginal detection we use this luminosity to derive an upper limit on the star formation rate, with SFR = $(1.4 \pm 0.4) \times 10^{-41} L_{\rm [OII]} \lesssim 0.1$ M$_\odot$ yr^{-1} (Kennicutt 1998). This is smaller than the star formation rates inferred for the star forming hosts of short GRBs (Berger 2009).

3.2. *Broad-band Photometry*

To extract additional information about the host galaxy we fit the broad-band photometry with Maraston (2005) evolutionary stellar population synthesis models. We use the subset of models described in Leibler & Berger (2010), with a Salpeter initial mass function, solar metallicity, and a red horizontal branch morphology, leaving redshift as a free parameter; see Figure 6. We find the best-fit solution to be $z = 0.75$ ($\chi^2_\nu = 0.3$ for 5 degrees of freedom) with a 2σ range of $z \approx 0.57 - 0.92$ (Figure 7), consistent with our spectroscopic redshift determination. Since $z = 0.75$ is ruled out at high confidence from the spectroscopic fit, we adopt $z = 0.915$ as the redshift of the host. At this redshift, the inferred stellar mass is 2.6×10^{10} M$_\odot$ and the stellar population age is about 1.1 Gyr, in good agreement with the spectroscopic results. The absolute B-band magnitude is M$_{\rm B} \simeq -20.3$ mag, corresponding to L$_{\rm B} \simeq 0.5$L$_*$ in comparison to the DEEP2 luminosity function at $z = 0.9$ (Willmer et al. 2006). We generally find poorer fits for models with 0.5 and 2 Z$_\odot$.

Combining the upper limit on the star formation rate with the inferred stellar mass, the resulting limit on the specific star formation rate is SSFR $\equiv$ SFR$/M_* \lesssim 0.004$ Gyr^{-1}. This confirms that the host galaxy is quiescent, since the characteristic growth timescale, SSFR$^{-1} \approx 260$ Gyr, is significantly larger than the Hubble time.

3.3. *Large-Scale Environment*

As shown in Figure 3, the field around GRB 100117A contains several red galaxies in addition to the host galaxy itself. We investigate whether the host and these galaxies are part of a large-scale structure similar to some previous short GRB environments (Bloom et al. 2006; Berger et al. 2007b), using color-color plots (Figure 8). We find that only one galaxy has similar colors to the host, and is therefore potentially located at the same redshift. Two additional galaxies have similar $r-J$ and $H-K$ colors to the host, with limits on their $g-r$ colors (due to g-band non-detections) that are consistent with the host of GRB 100117A. These galaxies may be less luminous members of the same large-scale structure. Additional spectroscopic observations are required to assess whether the host is part of a $z \approx 0.9$ galaxy group. However, we note that even if it is part of a real group, it is not a rich group or cluster.

4. GRB AND AFTERGLOW PROPERTIES

At the best-fit redshift of $z = 0.915$ the isotropic-equivalent γ-ray energy of GRB 100117A is $E_{\gamma,\rm iso} = 9.2 \times 10^{50}$ erg (16 – 2000 keV in the rest-frame). This is similar to the values inferred for previous short GRBs at a similar redshift (Berger et al. 2007a; Berger 2007, 2010a).

To extract additional information about the burst we use the measured brightness of the optical afterglow in conjunction with the limit on the X-ray flux (§2). The inferred optical to X-ray spectral index is $\beta_{\rm OX} \lesssim -0.75$, in agreement with the range of $\langle\beta_{\rm OX}\rangle = -0.72 \pm 0.17$ measured for short GRBs with X-ray and optical afterglow detections (Nysewander et al. 2009; Berger 2010a). Assuming the standard synchrotron emission spectrum from a relativistic blast wave (Sari et al. 1998), this value of $\beta_{\rm OX}$ indicates $p \gtrsim 2.5$ if $\nu_c > \nu_{\rm X}$, or $p \gtrsim 1.5$ if $\nu_c < \nu_{\rm O}$; here ν_c is the synchrotron cooling frequency and p is the power law index of the electron energy distribution, $N(\gamma) \propto \gamma^{-p}$. Since these values are not atypical, we cannot robustly locate ν_c based on the optical to X-ray flux ratio.

However, we can still constrain the circumburst density (n) by making the reasonable assumption that the cooling frequency is located above the optical band, while the synchrotron peak frequency, ν_m, is located below the optical band since the optical afterglow is fading at discovery. Using the observed optical afterglow brightness and assuming a constant density medium we find (Granot & Sari 2002):

$$n \approx 7.3 \times 10^{-12} \epsilon_e^{-3} \epsilon_B^{-1.75} E_{52}^{-2.75} \ {\rm cm}^{-3}, \quad (2)$$

where ϵ_e and ϵ_B are the fractions of energy in the radiating electrons and magnetic field, respectively, and E_{52} is the energy in units of 10^{52} erg. Assuming that $E \approx E_{\gamma,\rm iso}$ and using $\epsilon_e, \epsilon_B \lesssim 1/3$ we infer a lower limit on the density of $n \gtrsim 10^{-6}$ cm^{-3}, which is similar to IGM densities. For more typical values of $\epsilon_e \approx \epsilon_B \approx 0.1$, we find $n \approx 3 \times 10^{-4}$ cm^{-3}. Since generally $\epsilon_e, \epsilon_B \gtrsim 0.01$ (Panaitescu & Kumar 2002; Yost et al. 2003), a likely upper bound on the density is $n \lesssim 20$ cm^{-3}.

5. DISCUSSION AND CONCLUSIONS

In the sample of 14 short GRBs with optical afterglows and coincident hosts, GRB 100117A is only the second event unambiguously associated with an early-type galaxy (the other being GRB 050724; Berger et al. 2005). Additional cases of early-type hosts have been proposed. In particular, GRB 050509b is likely associated with an early-type cluster galaxy but this is based on only an X-ray position (Bloom et al. 2006). Two additional bursts (070809 and 090515) lack coincident hosts despite optical afterglow detections, but in both cases the galaxies with the lowest probability of chance coincidence are early-type galaxies (Berger 2010a). Even if we accept these additional early-type host associations as genuine, the host of GRB 100117A is located at a significantly higher redshift than the previous events, with $z \approx 0.23-0.47$. GRB 100117A also has the highest isotropic-equivalent gamma-ray energy of these events by a factor of a few, with $E_{\gamma,\rm iso} = 2.1 \times 10^{50}$ erg ($15-150$ keV). These results suggest that some of the optically-faint host galaxies identified to date (e.g., Berger et al. 2007a) may be bright near-IR sources due to a dominant old population. It also indicates that the presence of short GRBs in early-type galaxies does not necessarily point to progenitor ages of ~ 10 Gyr. Instead, the typical ages of short GRB progenitors in early-type hosts appear to be $\sim 1-4$ Gyr (Leibler & Berger 2010), which may lead to early-type hosts even at $z \approx 3$.

At the inferred redshift of $z = 0.915$ the projected physical offset of GRB 100117A is only 470 ± 310 pc. Our previous analysis of short GRB offsets revealed a median projected offset of about 5 kpc (Fong et al. 2010). In this context, GRB 100117A has the smallest offset measured to date. We note that the only other burst with a secure early-type host (GRB 050724) also has a small offset of about 2.7 kpc. Given the age of the stellar population of ~ 1 Gyr in both cases (see also Leibler & Berger 2010), these small offsets indicate that GRB 100117A and GRB 050724 did not originate from progenitors with a substantial kick (unless the kick direction in both cases is nearly aligned with our line of sight). Given the lack of any recent star formation activity, we can also rule out the possibility of a highly kicked progenitor system with a short merger time. On the other hand, the proposed associations of short GRBs 050509b, 070809, and 090515 with early-type hosts at offsets of tens of kpc (Bloom et al. 2006; Berger 2010a) indicates that some progenitors may experience large kicks. The cases of GRBs 070809 and 090515 is particularly intriguing since both had optical afterglows of comparable brightness to GRB 100117A (Figure 9), suggestive of a similar circumburst density despite a potential large difference in offsets.

Only a few short GRBs have circumburst density measurements, reflecting a general lack of multi-wavelength afterglow detections. GRB 051221A had an estimated density of $n \sim 10^{-3}$ cm^{-3} (Soderberg et al. 2006), GRB 050724 had $n \approx 0.01-0.1$ cm^{-3} (Berger et al. 2005), and GRB 050709 had[10] $n \lesssim 0.1$ cm^{-3} (Panaitescu 2006). For GRB 100117A we estimate $n \sim 10^{-4}-10$ cm^{-3}, continuing the trend of relatively low circumburst densities for short GRBs. This is particularly striking in comparison to the circumburst densities inferred for long GRBs, with a median of $\langle n \rangle \approx 1-10$ cm^{-3} (e.g., Soderberg et al. 2006).

Our discovery of the afterglow and $z = 0.915$ early-type host of GRB 100117A continues to support the conclusion that short GRBs exist at $z \sim 1$ and beyond (Berger et al. 2007a). However, unlike all previous short GRB hosts at these redshifts (Berger et al. 2007a; Graham et al. 2009; Antonelli et al. 2009; Levesque et al. 2010), the host of GRB 100117A exhibits no evidence for star formation activity and is instead dominated by a ~ 1 Gyr old stellar population. With its faint optical afterglow it is possible that previous such events have been missed due to shallow optical afterglows searches, thereby potentially biasing the known host population against $z \gtrsim 1$ early-type hosts.

We thank Rik Williams and Daniel Kelson for obtaining rapid observations of GRB 100117A with IMACS. This paper includes data gathered with the 6.5 meter Magellan Telescopes located at Las Campanas Observatory, Chile. Observations were also obtained at the Gemini Observatory, which is operated by the Association of Universities for Research in Astronomy, Inc., under a cooperative agreement with the NSF on behalf of the Gemini partnership: the National Science Foundation (United States), the Particle Physics and Astronomy Research Council (United Kingdom), the National Research Council (Canada), CONICYT (Chile), the Australian Research Council (Australia), CNPq (Brazil) and CONICET (Argentina). This work also made use of data supplied by the UK Swift Science Data Center at the University of Leicester. This work was partially supported by Swift AO5 grant #5080010 and AO6 grant #6090612.

[10] Only an upper bound is available due to the lack of a radio detection.

REFERENCES

Alard, C. 2000, A&AS, 144, 363
Antonelli, L. A., et al. 2009, A&A, 507, L45
Berger, E. 2007, ApJ, 670, 1254
Berger, E. 2009, ApJ, 690, 231
Berger, E. 2010a, ApJ, 722, 1946
Berger, E. 2010b, arXiv:1005.1068, New Astronomy Reviews in press
Berger, E., Cenko, S. B., Fox, D. B., & Cucchiara, A. 2009, ApJ, 704, 877
Berger, E., et al. 2007a, ApJ, 664, 1000
Berger, E., & Kelson, D. 2009, GRB Coordinates Network, 8934, 1
Berger, E., et al. 2005, Nature, 438, 988
Berger, E., Shin, M.-S., Mulchaey, J. S., & Jeltema, T. E. 2007b, ApJ, 660, 496
Bessell, M. S. 1999, PASP, 111, 1426
Bloom, J. S., et al. 2006, ApJ, 638, 354
Bruzual, G., & Charlot, S. 2003, MNRAS, 344, 1000
Cenko, S. B., Cobb, B. E., Perley, D. A., & Bloom, J. S. 2009, GRB Coordinates Network, 8933, 1
Cenko, S. B., Perley, D. A., Bloom, J. S., Cobb, B. E., & Morgan, A. N. 2010, GRB Coordinates Network, Circular Service, 339, 1 (2010), 339, 1
D'Avanzo, P., et al. 2009, A&A, 498, 711
de Pasquale, M., Markwardt, C., & Sbarufatti, B. 2010, GCN Report, 269, 1

de Ugarte Postigo, A., et al. 2006, ApJ, 648, L83
Evans, P. A., et al. 2009, MNRAS, 397, 1177
Evans, P. A., et al. 2007, A&A, 469, 379
Fong, W., Berger, E., & Fox, D. B. 2010, ApJ, 708, 9
Fox, D. B., et al. 2005, Nature, 437, 845
Graham, J. F., et al. 2009, ApJ, 698, 1620
Granot, J., & Sari, R. 2002, ApJ, 568, 820
Hjorth, J., et al. 2005a, ApJ, 630, L117
Hjorth, J., et al. 2005b, Nature, 437, 859
Kennicutt, R. C., Jr. 1998, ARA&A, 36, 189
Leibler, C. N., & Berger, E. 2010, ApJ, 725, 1202
Levan, A. J., et al. 2006, ApJ, 648, L9
Levesque, E. M., et al. 2010, MNRAS, 401, 963
Li, L.-X., & Paczyński, B. 1998, ApJ, 507, L59
Malesani, D., de Ugarte Postigo, A., Levan, A. J., Tanvir, N. R., Hjorth, J., & D'Avanzo, P. 2009, GRB Coordinates Network, Circular Service, 156, 1 (2009), 156, 1
Maraston, C. 2005, MNRAS, 362, 799
McBreen, S., et al. 2010, A&A, 516, A71
Metzger, B. D., et al. 2010, MNRAS, 406, 2650
Nysewander, M., Fruchter, A. S., & Pe'er, A. 2009, ApJ, 701, 824
Panaitescu, A. 2006, MNRAS, 367, L42
Panaitescu, A., & Kumar, P. 2002, ApJ, 571, 779
Perley, D. A., et al. 2009, ApJ, 696, 1871
Perley, D. A., Thoene, C. C., Cooke, J., Bloom, J. S., & Barton, E. 2007, GRB Coordinates Network, 6739, 1
Piranomonte, S., et al. 2008, A&A, 491, 183
Roming, P. W. A., et al. 2006, ApJ, 651, 985
Rowlinson, A., et al. 2010a, MNRAS, 408, 383
Rowlinson, A., et al. 2010b, MNRAS, 409, 531
Sari, R., Piran, T., & Narayan, R. 1998, ApJ, 497, L17
Soderberg, A. M., et al. 2006, ApJ, 650, 261
Stratta, G., et al. 2007, A&A, 474, 827
Willmer, C. N. A., et al. 2006, ApJ, 647, 853
Xu, D., Malesani, D., Leloudas, G., Fynbo, J. P. U., Djupvik, A. A., Karjalainen, R., Tanvir, N. R., & Jakobsson, P. 2010, GRB Coordinates Network, Circular Service, 337, 1 (2010), 337, 1
Yost, S. A., Harrison, F. A., Sari, R., & Frail, D. A. 2003, ApJ, 597, 459
Zheng, Z., & Ramirez-Ruiz, E. 2007, ApJ, 665, 1220

TABLE 1
LOG OF OPTICAL AND NEAR-IR AND OBSERVATIONS OF GRB 100117A

Date (UT)	Δt (d)	Telescope	Instrument	Filter	Exposures (s)	$\theta_{\rm FWHM}$ ($''$)	Afterglow[a] (AB mag)	F_ν^a (μJy)	Host[a] (AB mag)	A_λ^b (mag)
2010 Jan 18.040	0.162	Magellan	IMACS	*R*	4×300	1.25	>23.93	<0.97	···	0.064
2010 Jan 18.207	0.329	Gemini-North	GMOS	*r*	15×180	0.80	25.46 ± 0.20	0.24 ± 0.05	···	0.07
2010 Jan 19.262	1.383	Gemini-North	GMOS	*r*	15×180	0.76	···	0[c]	24.30 ± 0.10	0.07
2010 Feb 2.208	15.3	Gemini-North	NIRI	*K*	19×60	0.51			21.24 ± 0.20	0.01
2010 Feb 2.229	15.4	Gemini-North	NIRI	*H*	19×60	0.56			21.26 ± 0.21	0.01
2010 Feb 4.208	17.3	Gemini-North	NIRI	*J*	14×60	0.80			21.87 ± 0.25	0.02
2010 Feb 4.229	17.4	Gemini-North	GMOS	*g*	7×240	1.15			26.17 ± 0.30	0.1
2010 Nov 14.042	300.2	Magellan	IMACS	*z*	5×180	0.70			22.33 ± 0.10	0.035
2010 Nov 14.057	300.2	Magellan	IMACS	*i*	3×240	0.63			22.85 ± 0.10	0.045
2010 Nov 14.083	300.2	Magellan	IMACS	*r*	8×360	0.61			24.33 ± 0.10	0.07

NOTE. — [a] These values are corrected for Galactic extinction.
[b] Galactic extinction.
[c] We assume the afterglow contribution is negligible 1.383 d after the burst.

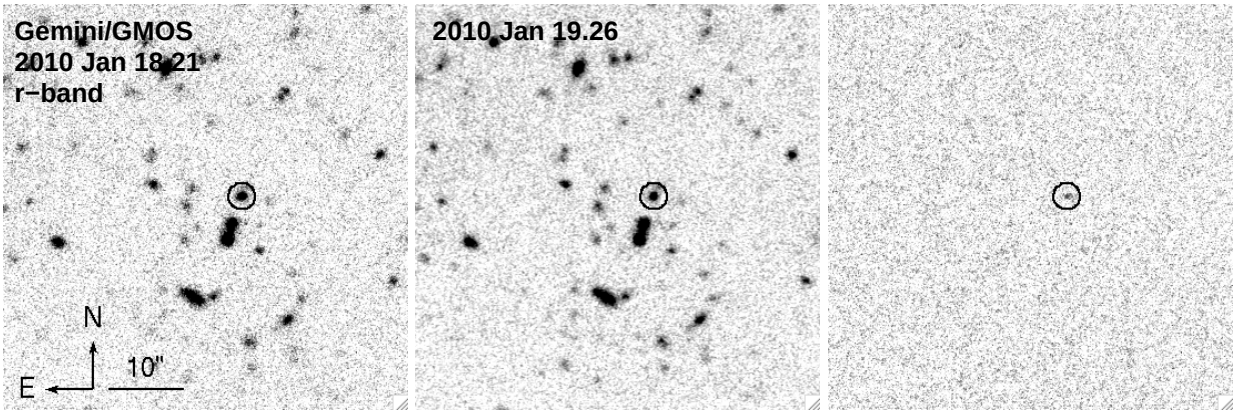


FIG. 1.— Gemini/GMOS *r*-band images obtained starting 7.9 hr (left) and 33.2 hr (center) after the burst. Digital subtraction of the two images reveals a fading source in the residual image (right), which we identify as the afterglow. The afterglow position is denoted by the black circle.

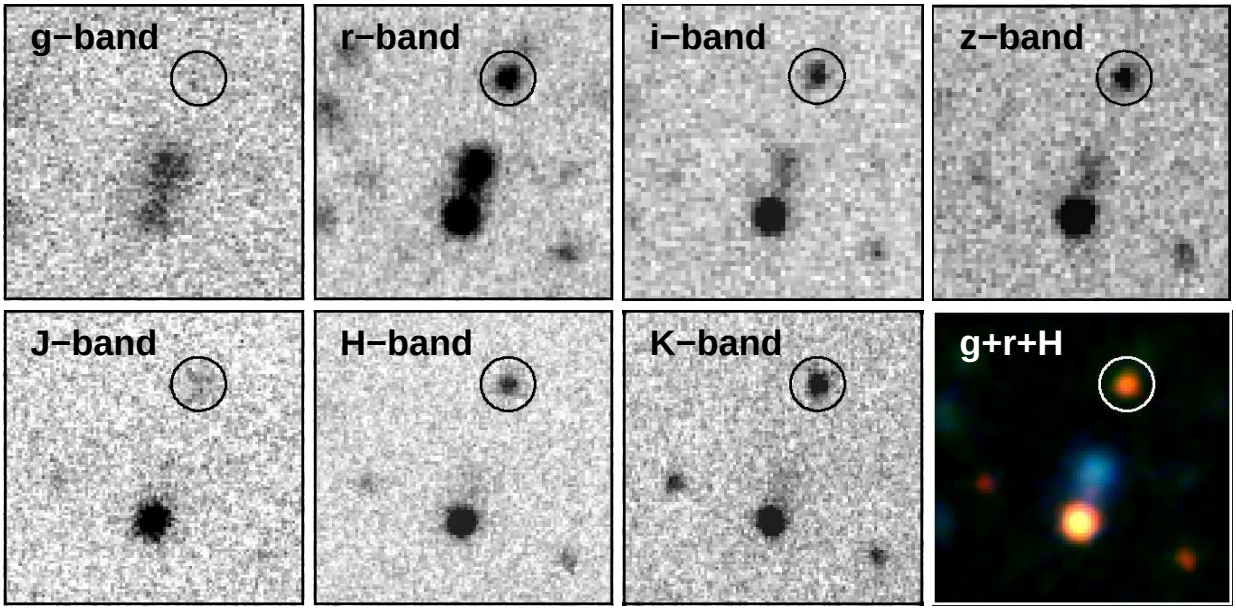


FIG. 2.— Gemini and Magellan optical and near-IR images of the host galaxy of GRB 100117A obtained with GMOS, NIRI and IMACS (Table 1). Each panel is 0.2′ on a side with an orientation of north up and east to the left. Also shown is a *grH* color composite highlighting the red color of the host galaxy.

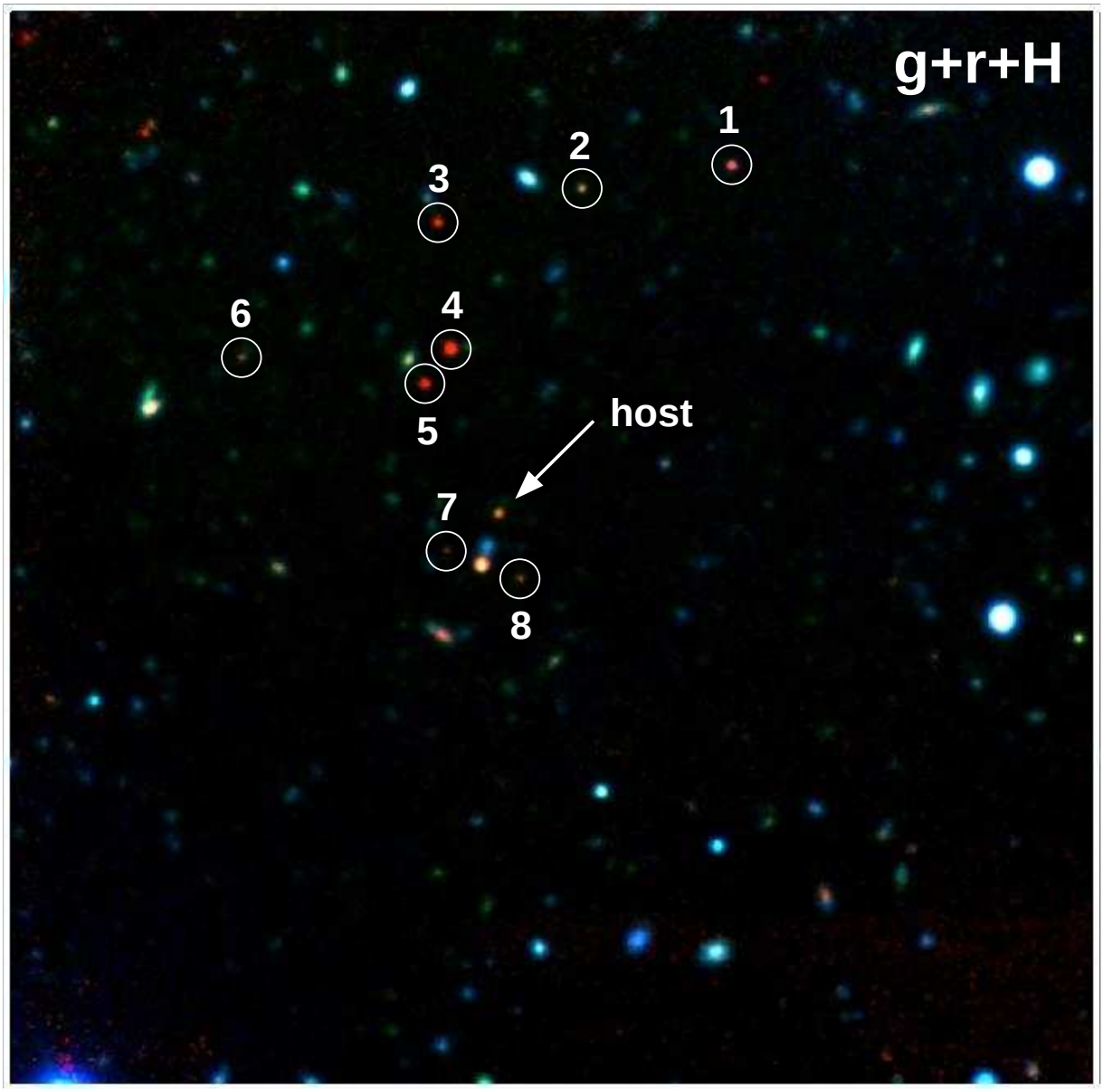


FIG. 3.— Gemini optical and near-IR *grH* color composite image of a $2' \times 2'$ field around GRB 100117A. The environment around the host contains several red galaxies, whose colors are plotted in Figure 8 (see §3.3).

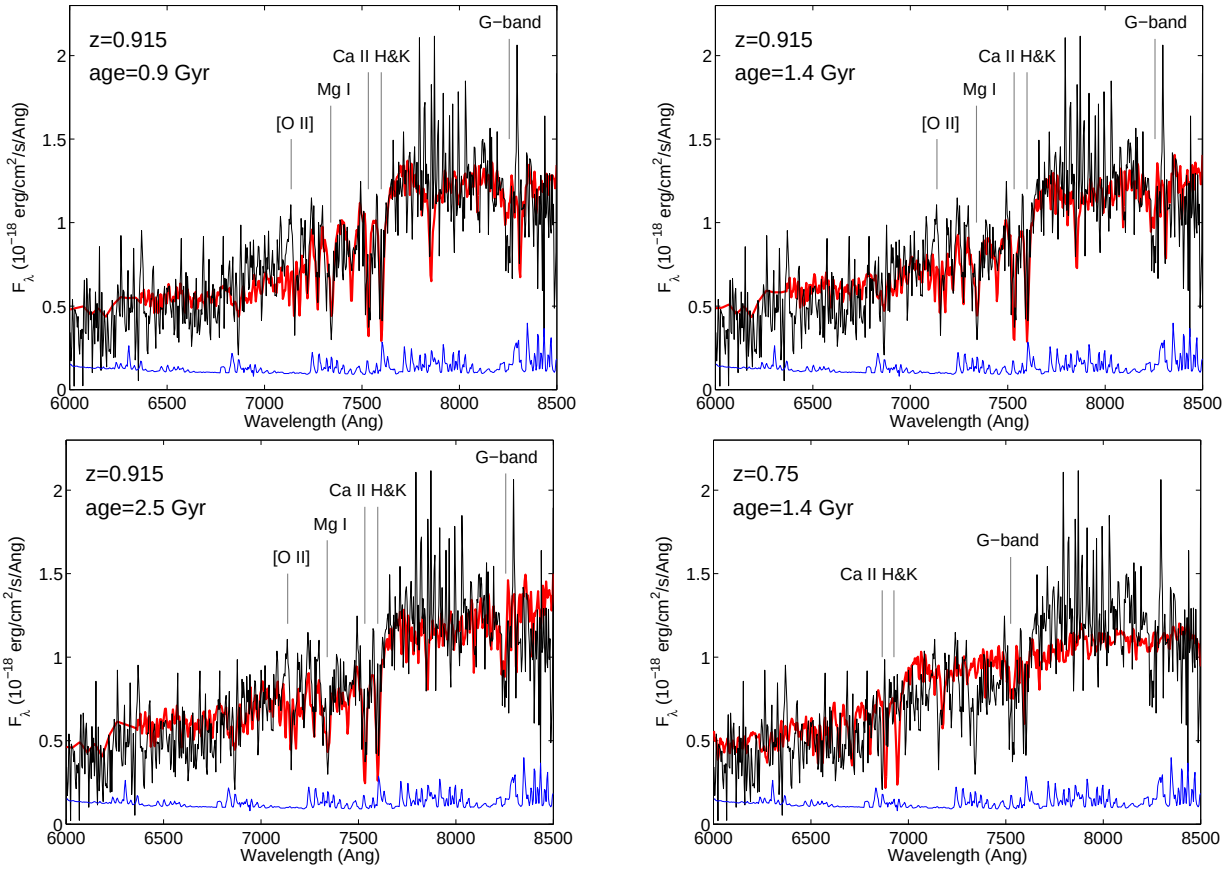


FIG. 4.— Gemini spectrum of the host galaxy of GRB 100117A binned with 3-pixel boxcar (black: data; blue: error spectrum). Also shown are SSP templates (red; Bruzual & Charlot 2003) with stellar population ages of 0.9 Gyr (top left), 1.4 Gyr (top right), and 2.5 Gyr (bottom left) at the best-fit spectroscopic redshift of $z = 0.915$. We also show a 1.4 Gyr SSP template at the preferred photometric redshift of $z = 0.75$ (bottom right). Fits are performed on the unbinned data. The latter fit provides a poorer match to both the sharpness of the break and the main spectral features. Absorption line locations corresponding to Ca II H&K, Mg Iλ3830, and G-bandλ4300 are indicated. Also shown is the expected location of the [O II]λ3727 emission doublet.

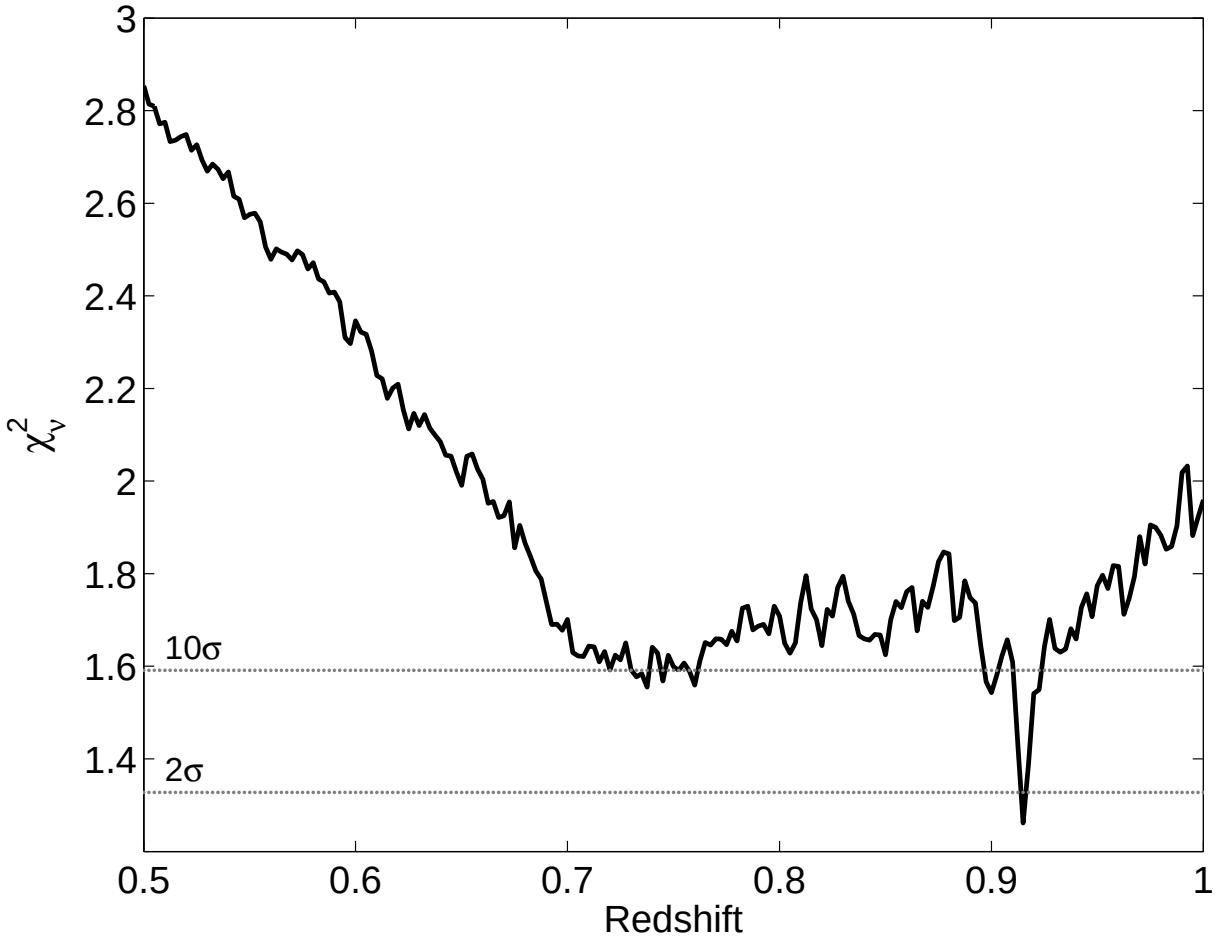


FIG. 5.— χ^2_ν as a function of redshift for the spectroscopic fit to a 1.4 Gyr SSP template (performed on the unbinned data, described in §3.1). The 2σ and 10σ levels are labeled. We find a sharp minimum at $z = 0.915$ with $\chi^2_\nu = 1.26$ and a broad minimum at $z \sim 0.75$, which is only consistent with the data at the 10σ level.

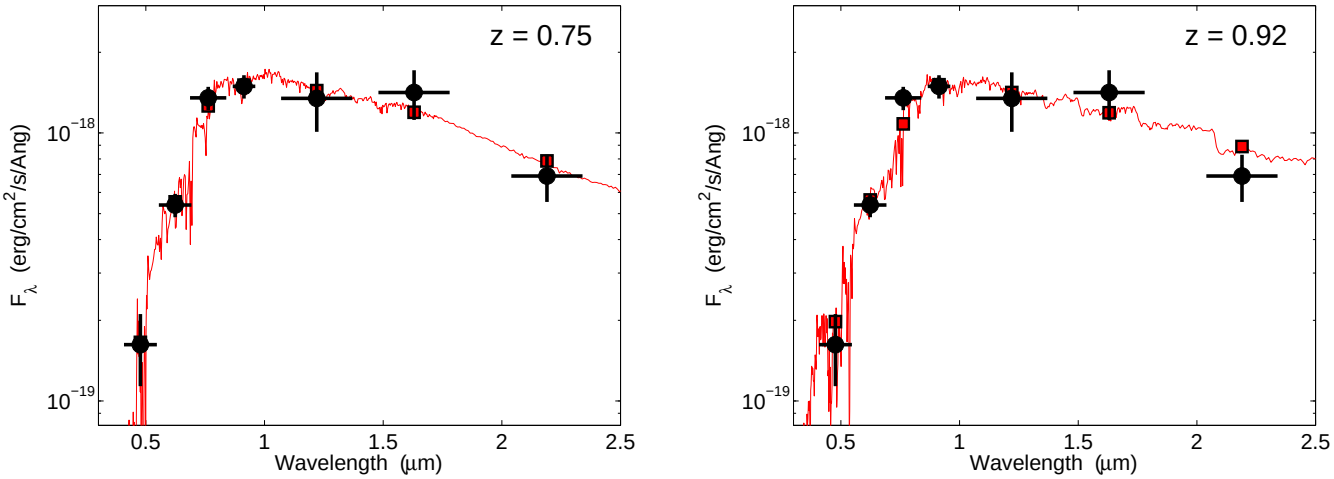


FIG. 6.— Optical and near-IR spectral energy distribution of the host galaxy of GRB 100117A (black circles). Each SED is fit with a Maraston (2005) single stellar population model (red line) through a maximum likelihood fit of the synthesized photometry (red squares, §3.2). We show the fits at the photometric best-fit $z = 0.75$ (left), and also at the preferred spectroscopic redshift $z = 0.915$ (right).

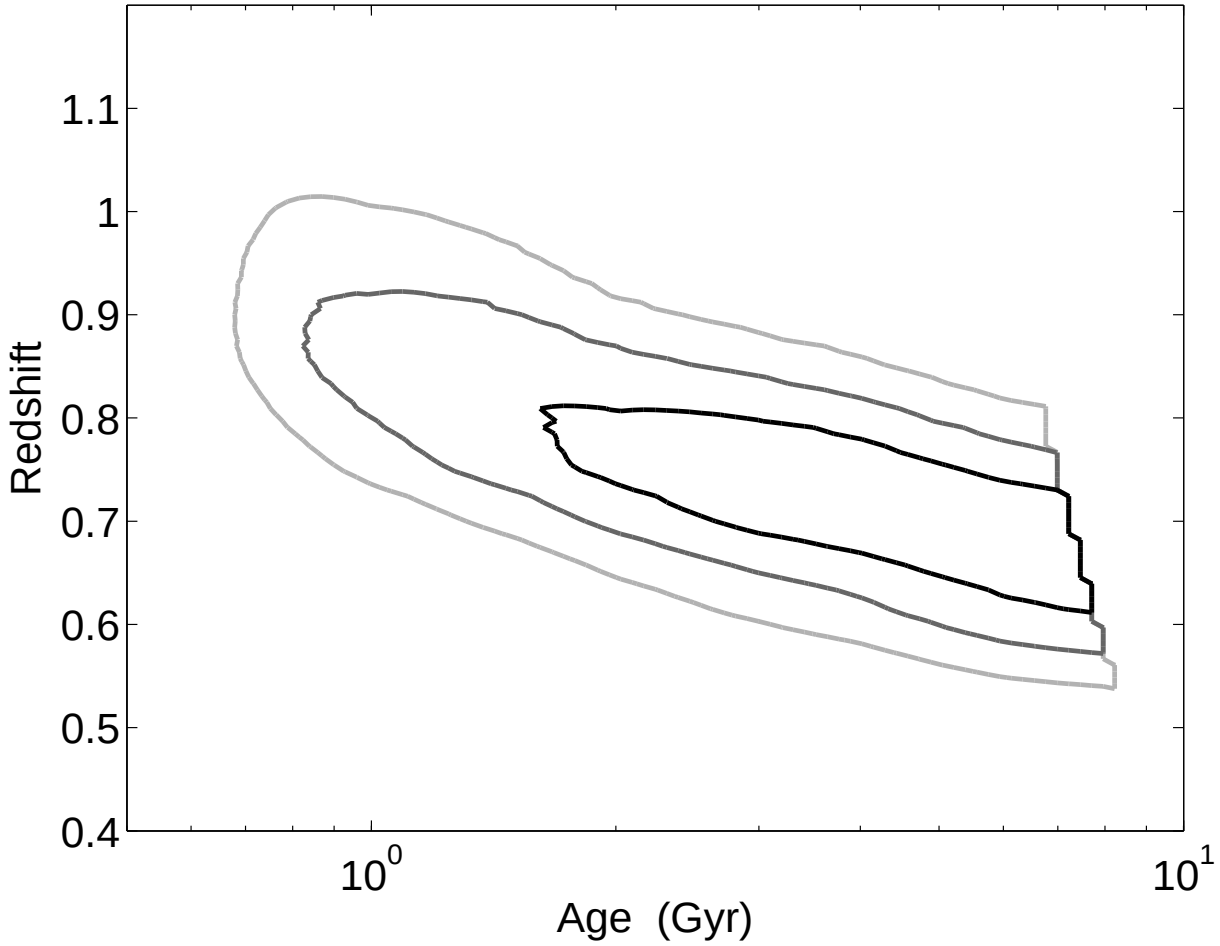


FIG. 7.— χ^2_ν contours for redshift and stellar population age using the Maraston (2005) single stellar population model ($1,2,3\sigma$ in order of decreasing darkness). The jagged edge at large ages is due to truncation at the appropriate age of the universe as a function of redshift. The 2σ contour leads to a best-fit redshift of $z = 0.57-0.92$.

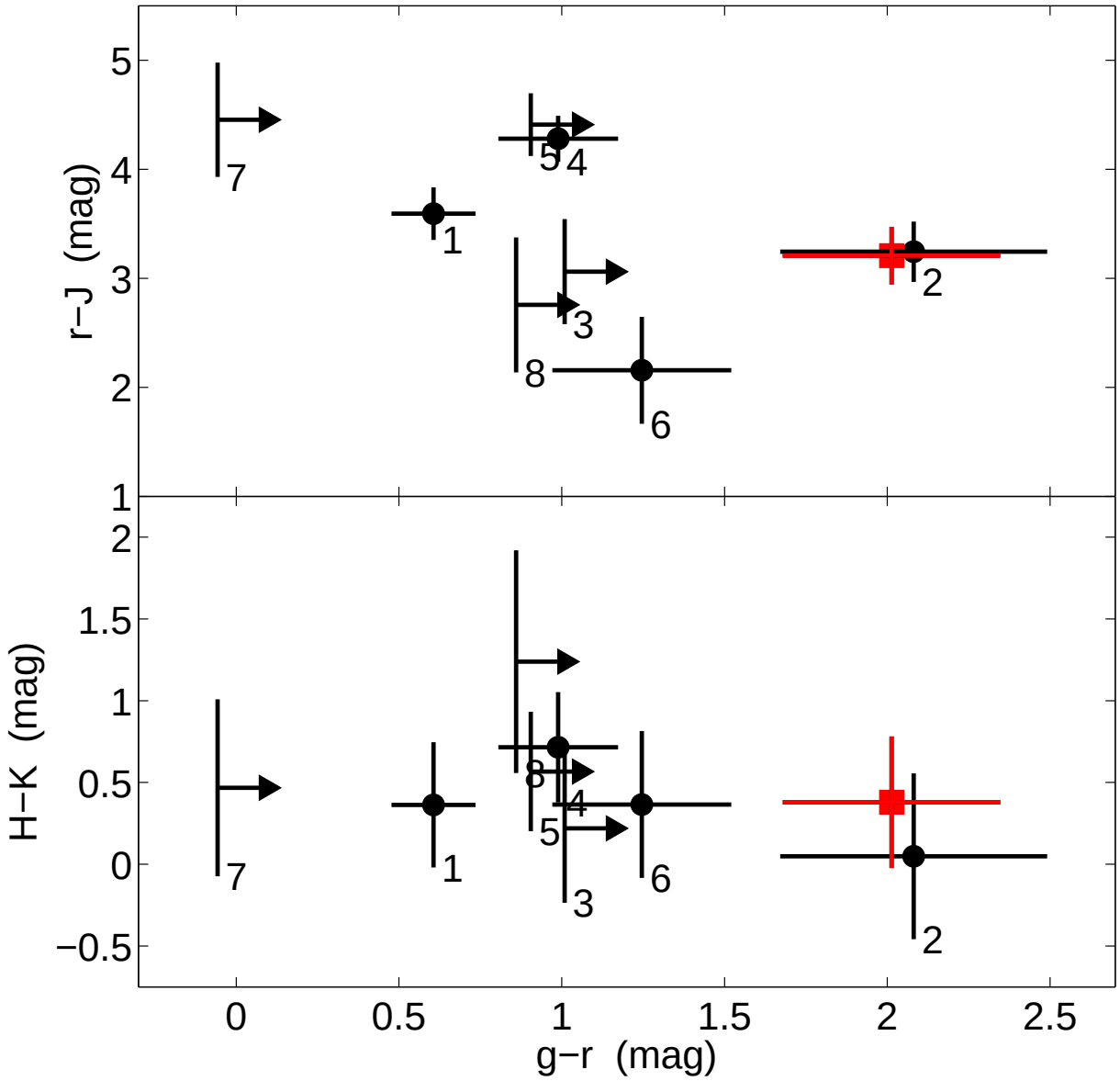


FIG. 8.— Color-color plots for red galaxies in a $2' \times 2'$ field around GRB 100117A (Figure 3). The host galaxy is marked by a red square. We identify an additional galaxy with similar colors (#2), and two potential galaxies with similar colors (although only lower limits in $g-r$; #3 and #8).

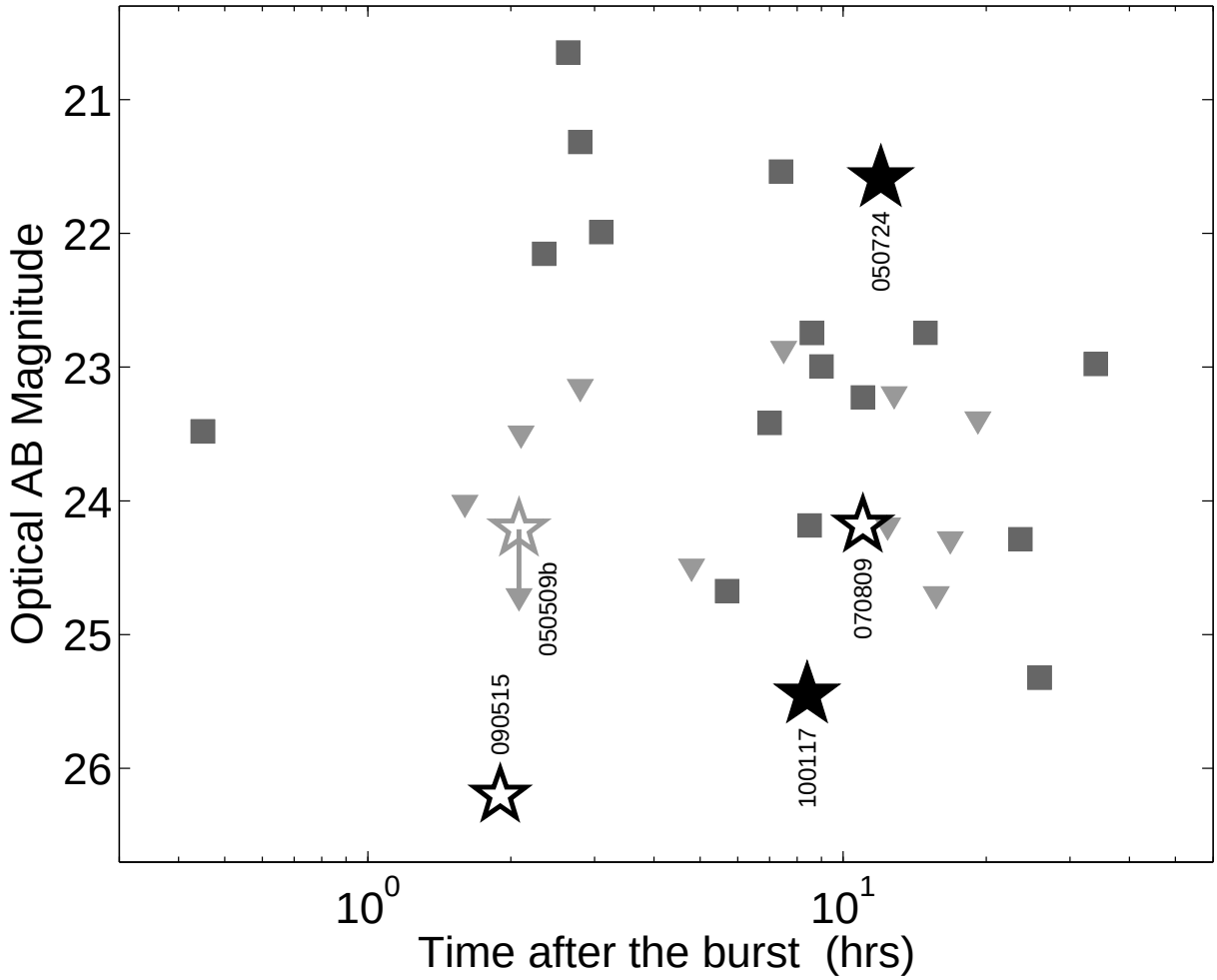


FIG. 9.— Short GRB optical afterglow brightness at the time of discovery for bursts with detected optical afterglows (squares) and upper limits (arrows). The two short GRBs with secure early-type hosts are denoted by solid stars, while bursts with putative early-type hosts are marked by open stars (Berger 2010a and references therein). Short GRBs with early-type hosts may have weaker optical afterglows on average, possibly related to lower circumburst densities.